JOURNAL OF APPLIED ELECTROCHEMISTRY 21 (1991) 583–587

Mass transfer and flow rate measurements for a system of two rotating disc electrodes with an axial electrolyte inlet

M. ŠIMEK

Fezko s.p., 386 16 Strakonice, Czechoslovakia

I. ROUŠAR

Department of Inorganic Technology, Institute of Chemical Technology, 166 28 Prague 6, Czechoslovakia

Received 24 October 1989; revised 20 November 1990

Limiting currents and volume flow rates in the self pumping regime were measured on a model rotating electrolyzer with a variable geometry. The volume flow rate depends not only on the radius of the inlet orifice, outer disc radius, and angular velocity, but also on the interelectrode distance. Experimental mean current densities are compared with those calculated by the finite-element method, from an equation based on the theory of similarity of the diffusion layer, and from the theory of the rotating disc electrode with a ring.

Notation

a_1–a_4	constants
c_0	bulk concentration
D	diffusion coefficient
F	Faraday constant, 96 487 C mol^{-1}
h	interelectrode distance
I	current
$\bar{j}$	mean current density
k_1, k_2	constants
n	number of transferred electrons
Q	volume rate of flow
r	radial coordinate
r_0	inner radius of electrode
r_1	outer radius of electrode
r_v	radius of inlet orifice
r_d	outer radius of disc
R	radius of measuring tube
u_{max}	maximum velocity of liquid
z	normal coordinate
η	dynamic viscosity
ν	kinematic viscosity
ρ	density
ω	angular velocity

1. Introduction

An electrolyzer with two rotating, parallel disc electrodes with an axial electrolyte inlet is denoted in the literature as a rotating electrolyzer [1]. One electrode is provided with a central opening for the electrolyte inlet [2]. The discs are electrically insulated from each other and attached to a common axis. This system has been investigated both theoretically and practically by a number of authors [1–5]; its description and a survey of results is given in our earlier work [6].

The method of similarity of the diffusion layer was used for electrodes placed at a sufficient distance from the rotation axis to obtain the following analytical expression for the mean current density [6]:

$$\bar{j} = 0.544nFD^{2/3}c_0(\omega Q/\nu)^{1/3}(r_1^2 - r_0^2)^{-1/3} \quad (1)$$

For electrodes placed nearer to the rotation axis, the current density is obtained from a numerical solution of the convective diffusion equation, e.g. by a finite-element method [6].

In order to obtain further data for the rotating electrolyzer the volume rates of flow and the mean limiting current densities were measured on systems with variable geometry in the self pumping regime. A comparison of the measured data with the theory is presented.

2. Description of the model system

The model electrolyzer is shown schematically in Fig. 1. It consists of two iron disc electrodes of outer radius r_d (60, 80, or 100 mm), 2 mm in thickness and nickel plated, which are mechanically connected in the central region by three hollow spacers (25 mm apart from the centre; spacer diameter 6 mm) allowing a firm connection of the two discs by means of screws. Six other spacers of a non-conducting material were placed on the periphery of the disc (5 mm from the outer limit, spacer diameter 4 mm); these were as long as the inner spacers and ensured planarity of the system. The interelectrode distance was h = 3.7, 6.2, or 8.7 mm. The lower disc was provided with a circular opening of radius r_v = 10, 15, or 20 mm, and the upper was fastened by two screws to the transmission shaft driven by an electric motor. The rotation rate

0021-891X/91 $03.00 + .12

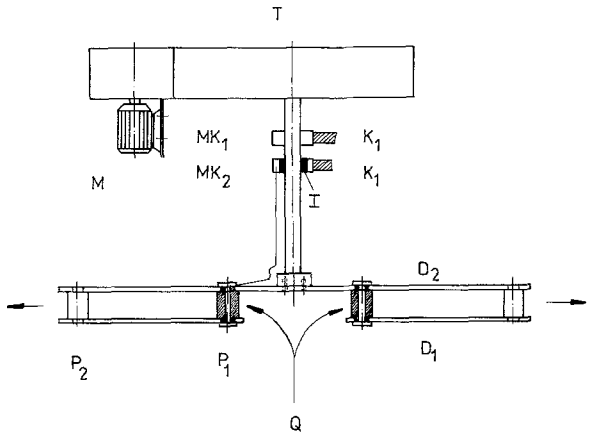

Fig. 1. Scheme of a model rotating electrolyzer. D_1 lower disc, D_2 upper disc, I insulation, K_1 contact to the lower electrode, K_2 contact to the upper electrode, M electric motor, MK_1 and MK_2 copper rings, P_1 inner spacers, P_2 outer spacer, T transmission; the direction of streaming is indicated by arrows.

could be varied in 18 steps from 15.5 to 262 r.p.m. The electrode surface on each disc was delimited by the radii r_0 and r_1, the remaining surface being provided with an insulating layer of an epoxy resin. Four combinations of r_0 and r_1 values were chosen: 35 and 50 mm, 35 and 70 mm, 40 and 80 mm, and 50 and 80 mm, respectively.

3. Measurement of the flow rate

The volume flow rate was measured in an experimental set-up according to Fig. 2. A thin-walled aluminium tube of 40 mm inner diameter provided with an insulating epoxy resin coating was fastened by a screw to the lower disc; the tube reached into a container filled with mercury acting as a siphon. When the discs were set into rotation, the liquid was sucked from a longer vertical tube of 50 mm inner diameter, whose upper part was provided with a conical insert so as to gradually diminish the inner diameter to 25 mm at the upper end (angle of the cone wall about 7.5°). The meausring zone was preceded by a 'calming' zone 55 cm in length. Thus, a parabolic velocity profile was attained in the measuring zone with the maximum velocity in the centre. This quantity was measured by injecting an indicator into the stream using a small 2 cm^3 syringe. As soon as the indicator reached the first platinum indicator electrode in the centre of the tube, the electrode potential changed and a peak was obtained. As soon as the indicator reached the second platinum electrode in the channel centre, its potential changed and another peak was recorded. From the chart speed and the mutual distance of the two peaks the velocity of the liquid in the centre was calculated (u_{max}). If the velocity profile is fully developed, the volume rate of flow is given as

$$Q = \pi u_{max} R^2/2 \qquad (2)$$

where R denotes radius of the measuring tube, i.e. 25 mm.

The measurement was carried out with a solution of 0.3 M $K_4Fe(CN)_6$ and 0.5 M KOH. The indicator sol-

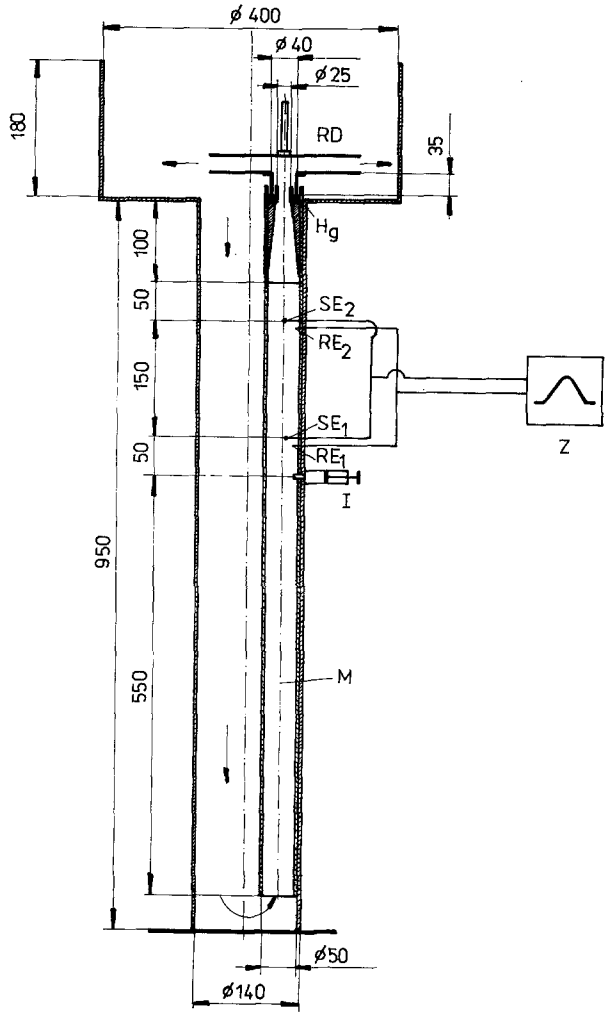

Fig. 2. Scheme of the equipment for measurement of the rate of flow. I syringe, M measuring tube, RD rotating discs, RE reference electrode, SE sensing electrode, Z recorder; the flow direction is indicated by arrows.

ution was 0.05–0.3 M $K_3Fe(CN)_6$ and the injected quantity was 0.1–0.2 cm^3. The change of the redox potential difference between the indicator electrodes was 5–40 mV. The total volume of liquid in the equipment was 241. The solution was replaced by a fresh one if the changes of the redox potential became smaller than 5 mV (due to contamination of the solution with $K_3Fe(CN)_6$). The temperature of measurement was 25 ± 0.5° C. Some time was allowed to elapse prior to every measurement in order to attain a steady velocity profile in the tube.

4. Measurement of the mass transfer

During measurement of the mass transfer, each electrode was electrically connected with a copper ring on the shaft, provided with a sliding contact (Fig. 1). The discs were immersed in a cylindrical vessel of 35 cm radius filled with the electrolyte, which was repelled by rotation from between the discs. The solution composition was 0.0300 M $K_3Fe(CN)_6$, 0.300 M $K_4Fe(CN)_6$ and 0.500 M KOH. The physical parameters at 25.0 ± 0.1° C were: density ρ = (1.0924 ± 0.0009) × 10^{-3} kg cm^{-3}, dynamic viscosity η = (1.08 ± 0.01) × 10^{-5} kg cm s^{-1}, kinematic viscosity

$\nu = (0.99 \pm 0.01) \times 10^{-2}\,cm^2\,s^{-1}$, diffusion coefficient of $[Fe(CN)_6]^{3-}$ $D = (6.38 \pm 0.04) \times 10^{-6}\,cm^2\,s^{-1}$. The total volume of the solution was 10 l. The solution was used for no more than three days.

The chosen system has the advantage that the electrode reactions are sufficiently rapid, so that limiting current is easily measurable, and that the solution composition remains unchanged during electrolysis in the region of the limiting current. The course of the polarization curves showed that it was preferable to measure the cathodic limiting current (reduction of $[Fe(CN)_6]^{3-}$ to $[Fe(CN)_6]^{4-}$, which was sufficiently constant over a wide potential range (350–800 mV) at a ratio of the concentrations of $[Fe(CN)_6]^{4-}$ to $[Fe(CN)_6]^{3-}$ of 10:1. An excess of the reduced form was chosen in order that the limiting current be governed only by diffusion of $[Fe(CN)_6]^{3-}$ to the cathode. Under these conditions it is possible, by a change of polarity of the electrodes, to find whether the velocity profile is symmetrical with respect to the central plane between the discs or not. In the case of a symmetrical profile, the cathodic limiting currents on the two disc electrodes must be equal.

The measured limiting current on an electrode with radii r_0 and r_1 was used to calculate the mean current density as

$$\bar{j} = I/\pi(r_1^2 - r_0^2). \tag{3}$$

The nickel-plated electrode surface was thoroughly rinsed with toluene before the first measurement to remove residues of polishing agents, and it was further rinsed with 10% H_2SO_4 and with distilled water prior to immersing in the electrolyte. This procedure ensured reproducible results.

5. Results of measurement of the volume flow rate

For each chosen geometry, the rate of flow was measured at 6 to 18 different angular velocities. Each result is an average from at least five measurements with as many injections of the indicator solution; the volume flow rate was calculated from Equation 2. The results were correlated with the angular velocity in [5] according to the expression

$$Q = k_1\omega^{k_2} \tag{4}$$

This equation holds good over a certain interval of ω values. For larger discs ($r_d = 100$ mm), deviations from the linear dependence of log Q on log ω are observed at high angular velocities and hence at high flow rates. This is due to a change in the measuring tube from laminar to turbulent flow. If the volume flow rate is recalculated on the assumption of a fully developed turbulent velocity profile [7] at a high value of ω, it satisfies Equation 4.

The constants k_1 and k_2 were calculated in the laminar streaming region by the least squares method and are given in Table 1 (correlation coefficient was higher than 0.999). The value of k_2 is close to 1, corresponding to the theory of hydrodynamic pumps [8].

The pumping stability of the apparatus is considerable; it is mainly controlled by the surface area of the discs, causing transfer of momentum from the discs into the liquid. Thus, a larger surface area causes a higher rate of flow. On the other hand, decreasing the inlet orifice radius and decreasing interelectrode distance cause the rate of flow to decrease. This is due to increasing hydrodynamic resistance, causing pressure losses.

With regard to the geometrical parameters of the system, the volume flow rate, Q ($cm^3\,s^{-1}$) can be described by the equation

$$Q = (0.038 \pm 0.007)(r_d^2 - r_v^2)r_d(h/r_d)^{0.08}(r_v/r_d)^{0.60} \tag{5}$$

with a relative error of 18.4%; the units used are centimetres and seconds. This equation holds for a model apparatus according to Fig. 1, r_d from 6 to 10 cm, r_v from 1 to 2 cm, h from 0.37 to 0.87 cm, and ω from 1.67 to 27.7 s^{-1}; the solution used was 0.3 M $K_4Fe(CN)_6$ + 0.5 M KOH at 25 ± 0.5° C. For other systems differing from that shown in Fig. 1, another equation would be necessary.

Table 1. Geometrical parameters and calculated constants k_1 and k_2 for Equation 4 with the upper limit of measured ω (ω_{max})

r_v (mm)	r_d (mm)	h (mm)	k_1 ($cm^3\,s^{-1}$)	k_2	ω_{max} (s^{-1})
20.0	100.0	3.7	10.5 ± 0.2	0.93 ± 0.01	10.0
		8.7	11.6 ± 0.2	0.93 ± 0.01	9.3
10.0	100.0	3.7	8.1 ± 0.2	0.97 ± 0.01	12.0
		8.7	9.1 ± 0.5	0.95 ± 0.04	10.0
20.0	80.0	3.7	6.0 ± 0.2	0.98 ± 0.01	14.7
		8.7	6.3 ± 0.1	0.98 ± 0.01	14.7
10.0	80.0	3.7	4.7 ± 0.2	0.98 ± 0.02	18.3
		8.7	5.2 ± 0.2	0.98 ± 0.02	18.3
20.0	60.0	3.7	3.38 ± 0.09	0.99 ± 0.01	27.7
		8.7	3.70 ± 0.09	0.98 ± 0.01	21.1
10.0	60.0	3.7	2.93 ± 0.08	0.99 ± 0.01	27.7
		6.2	3.5 ± 0.2	0.99 ± 0.02	27.7

6. Results of measurement of mean current densities

Measurements of the cathodic limiting currents on both discs substantiated the assumption that the flow is symmetrical with respect to the central plane (the limiting currents on both electrodes were equal in most cases, their relative difference not exceeding 2%). Altogether 50 different geometries of the system were studied at angular velocities varying from 1.67 to 27.7 s^{-1}. It was found that the dependence of the mean current density on ω can be expressed by the equation

$$\bar{j} = a_3\omega^{a_4} \tag{6}$$

The exponent a_4 ranges from 0.55 to 0.60, increasing somewhat with the distance of the electrode from the centre. By comparison of the dependences of $\bar{j}$ and the

Table 2. Coefficients a_3 and a_4 for Equation 6 approximating the mean current density obtained experimentally, calculated by the finite-element method and from Equation 1 for an electrode located far from the centre: $r_0 = 35$ mm, $r_1 = 50$ mm, $\omega = 1.62$–$27.7\ s^{-1}$. Equation 7 for a rotating ring disc: $a_3 = 1.964\ mA\ cm^{-2}$, $a_4 = 0.5$

r_d (mm)	r_v (mm)	h (mm)	Experiments		Numerical calculations		Equation 1	
			a_3 ($mA\ cm^{-2}$)	a_4	a_3 ($mA\ cm^{-2}$)	a_4	a_3 ($mA\ cm^{-2}$)	a_4
100.0	20.0	3.7	1.85 ± 0.04	0.557 ± 0.009	2.04 ± 0.08	0.52 ± 0.03	2.32	0.64
	10.0	3.7	1.78 ± 0.04	0.56 ± 0.01	1.96 ± 0.06	0.54 ± 0.02	2.13	0.66
	10.0	8.7	1.78 ± 0.04	0.56 ± 0.01	1.98 ± 0.03	0.54 ± 0.01	2.20	0.65
60.0	20.0	3.7	1.66 ± 0.03	0.565 ± 0.08	1.65 ± 0.04	0.59 ± 0.01	1.59	0.66
	10.0	3.7	1.67 ± 0.08	0.54 ± 0.02	1.58 ± 0.03	0.59 ± 0.01	1.52	0.66

Table 3. Coefficients a_3 and a_4 for Equation 6; electrode parameters $r_0 = 35$ mm, $r_1 = 70$ mm, other data as in Table 2. Equation 7: $a_3 = 1.617\ mA\ cm^{-2}$, $a_4 = 0.5$

r_d (mm)	r_v (mm)	h (mm)	Experiments		Numerical calculations		Equation 1	
			a_3 ($mA\ cm^{-2}$)	a_4	a_3 ($mA\ cm^{-2}$)	a_4	a_3 ($mA\ cm^{-2}$)	a_4
100.0	20.0	3.7	1.44 ± 0.02	0.576 ± 0.005	1.48 ± 0.04	0.58 ± 0.02	1.63	0.65
	10.0	3.7	1.37 ± 0.02	0.583 ± 0.006	1.37 ± 0.03	0.61 ± 0.01	1.50	0.66
80.0	20.0	3.7	1.34 ± 0.02	0.572 ± 0.007	1.31 ± 0.03	0.60 ± 0.01	1.35	0.66
	10.0	3.7	1.27 ± 0.02	0.576 ± 0.009	1.25 ± 0.02	0.603 ± 0.009	1.25	0.66

rate of flow it follows that both these quantities depend in the same manner on the geometries parameters, hence $\bar{j}$ is a certain function of the volume rate of flow. It was also found that the mean limiting current density depends on the interelectrode distance, h, over a certain range.

Numerical calculation by the finite-element method with approximation of the velocity field by functions of up to the third order [6] involving the volume flow rate from Equation 4 (with constants k_1 and k_2 from Table 1) gave the mean current densities which are, for larger distances of the electrode from the centre ($r_0 = 50$ mm), in agreement with the measured values (the error not exceeding 5%). For systems with electrodes nearer to the rotation axis (35 mm $\leqslant r_0 <$ 50 mm) the error does not exceed 10%.

A fair estimation of the mean current densities for volume rates of flow up to 150 $cm^3\ s^{-1}$ can be obtained from the equation for a rotating disc electrode with a ring [9] in the form

$$\bar{j} = 0.621nF(r_1^3 - r_0^3)^{2/3} c_0 D^{2/3} \nu^{-1/6} \omega^{1/2} / (r_1^2 - r_0^2) \quad (7)$$

A drawback of this equation is that it ignores the dependence of $\bar{j}$ on the volume flow rate observed experimentally.

The approximate expression, Equation 1, obtained from the theory of similarity of the diffusion layer leads to mean current densities which are, at $\omega = 27.7\ s^{-1}$, for most system geometries (by 30 or more percent) higher than the experimental values. The values of a_3 and a_4 obtained by correlation with the experimental data, with results calculated by the finite-

Table 4. Coefficients a_3 and a_4 for Equation 6; electrode parameters $r_0 = 40$ mm, $r_1 = 80$ mm, other data as in Table 2. Equation 7: $a_3 = 1.617\ mA\ cm^{-2}$, $a_4 = 0.5$

r_d (mm)	r_v (mm)	h (mm)	Experiments		Numerical calculations		Equation 1	
			a_3 ($mA\ cm^{-2}$)	a_4	a_3 ($mA\ cm^{-2}$)	a_4	a_3 ($mA\ cm^{-2}$)	a_4
100.0	20.0	3.7	1.38 ± 0.02	0.581 ± 0.008	1.42 ± 0.03	0.58 ± 0.01	1.49	0.65
		8.7	1.43 ± 0.03	0.577 ± 0.009	1.46 ± 0.02	0.579 ± 0.008	1.55	0.64
	15.0	3.7	1.33 ± 0.03	0.58 ± 0.01	1.38 ± 0.02	0.591 ± 0.008	1.46	0.65
		6.2	1.37 ± 0.03	0.58 ± 0.01	1.41 ± 0.02	0.583 ± 0.009	1.47	0.65
	10.0	3.7	1.28 ± 0.02	0.585 ± 0.009	1.33 ± 0.02	0.596 ± 0.009	1.37	0.66

Table 5. Coefficients a_3 and a_4 for Equation 6; electrode parameters r_0 = 50 mm, r_1 = 80 mm, other data as in Table 2. Equation 7: a_3 = 1.805 mA cm^{-2}, a_4 = 0.5

r_d (mm)	r_v (mm)	h (mm)	Experiments		Numerical calculations		Equation 1	
			a_3 (mA cm^{-2})	a_4	a_3 (mA cm^{-2})	a_4	a_3 (mA cm^{-2})	a_4
100.0	20.0	3.7	1.54 ± 0.02	0.582 ± 0.007	1.57 ± 0.03	0.580 ± 0.008	1.59	0.65
		8.7	1.61 ± 0.02	0.571 ± 0.007	1.63 ± 0.02	0.569 ± 0.005	1.66	0.64
	15.0	3.7	1.48 ± 0.03	0.588 ± 0.009	1.52 ± 0.02	0.585 ± 0.005	1.57	0.65
		8.7	1.53 ± 0.02	0.582 ± 0.006	1.58 ± 0.03	0.578 ± 0.008	1.58	0.64
	10.0	3.7	1.41 ± 0.02	0.596 ± 0.007	1.42 ± 0.02	0.601 ± 0.006	1.47	0.66
		8.7	1.45 ± 0.02	0.594 ± 0.007	1.49 ± 0.02	0.590 ± 0.005	1.52	0.65

element method, and from Equations 1 and 7 are given in Tables 2–5.

The calculated and measured limiting current densities for one of the studied systems are compared graphically in Fig. 3. The slope of the dependence of $\bar{j}$ on ω was constant even at the highest angular velocities in all the systems studied, hence a significant change from laminar to turbulent flow is improbable.

7. Conclusions

The measured volume flow rates can be correlated with the angular velocities by Equation 4 for all geometries considered with the constants k_1 and k_2 given in Table 1. The volume flow rate Q can be correlated with geometrical parameters of the system and angular velocity by Equation 5.

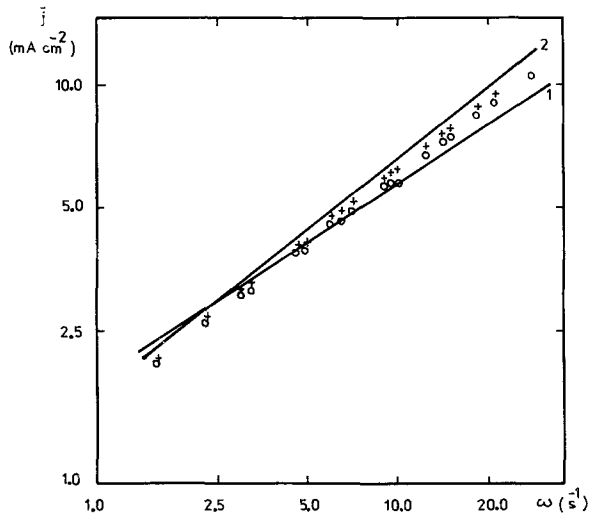

Fig. 3. Dependence of mean current density, $\bar{j}$, on angular velocity ω in logarithmic coordinates. System parameters: r_v = 20 mm, r_0 = 50 mm, r_1 = 80 mm, r_d = 100 mm, h = 3.7 mm; (O) measured values, (×) numerical calculation by the finite-element method; (1) Equation 7 for a rotating ring disc electrode, (2) Equation 1 for an electrode located far from the rotation axis.

The measured mean limiting cathodic current densities, $\bar{j}$, are best approximated by the numerical solution of the convective diffusion equation obtained by the finite-element method, the error not exceeding 10% (2–5% on the average). At volume flow rates up to 150 cm^3 s^{-1}, $\bar{j}$ can be approximated by Equation 7, valid for a rotating disc electrode with a ring [9].

Although Equation 1, obtained from the theory of similarity of the diffusion layer, is for ω = 27.7 s^{-1}, subject to errors of 30% or more, it is interesting since it predicts the dependence of $\bar{j}$ on the volume flow rate, which was substantiated experimentally. The agreement with experiments is better for electrodes located a larger distance from the rotation axis (r_0 = 50 mm, r_1 = 80 mm), and worse for those located nearer (r_0 = 35 mm, r_1 = 50 mm). Hence, Equation 1 holds good for electrodes located far from the rotation axis, which corresponds to the assumptions inherent in its derivation.

Note

Tables presented herein are shortened. Full data may be obtained directly from the authors.

References

[1] R. E. W. Jansson, *Electrochim. Acta* **23** (1978) 1345.
[2] M. Fleischmann, R. E. W. Jansson and R. J. Marshall, Brit. Pat. 04939 (1976).
[3] R. E. W. Jansson and R. J. Marshall, *J. Appl. Electrochem.* **8** (1978) 287.
[4] M. Šimek and I. Roušar, *Coll. Czech. Chem. Comm.* **49** (1984) 1122.
[5] A. B. Ferriera and R. E. W. Jansson, *Trans. Inst. Chem. Engnrs* **57** (1978) 262.
[6] M. Šimek and I. Roušar, *J. Appl. Electrochem.* **21** (1991) 111.
[7] H. Schlichting, 'Teoriya pogranichnogo sloya', Nauka, Moscow (1974).
[8] J. Bláha and K. Brada, 'Hydrodynamická čerpadla', ČVUT, Prague (1985).
[9] W. J. Albery and M. L. Hitchman, 'Ring-disc Electrode', Clarendon Press, Oxford (1971).